ACS Medicinal Chemistry Letters

pubs.acs.org/acsmedchemlett Letter

Leveraging Open Science Drug Development for PET: Preliminary Neuroimaging of ^{11}C-Labeled ALK2 Inhibitors

Emily Murrell, Junchao Tong, David Smil, Taira Kiyota, Ahmed M. Aman, Methvin B. Isaac, Iain D. G. Watson,* and Neil Vasdev*

Cite This: ACS Med. Chem. Lett. 2021, 12, 846−850 Read Online

ACCESS | Metrics & More | Article Recommendations | Supporting Information

ABSTRACT: Mutations in the gene encoding activin receptor-like kinase 2 (ALK2) are implicated in the pathophysiology of a pediatric brainstem cancer, diffuse intrinsic pontine glioma (DIPG). Inhibitors of ALK2 that cross the blood−brain barrier have been proposed as a method of treatment for DIPG. As part of an open science approach to radiopharmaceutical and drug discovery, we developed ^{11}C-labeled radiotracers from potent and selective lead ALK2 inhibitors to investigate their brain permeability through positron emission tomography (PET) neuroimaging. Four radiotracers were synthesized by ^{11}C-methylation and assessed by dynamic PET imaging in healthy Sprague−Dawley rats. One of the compounds, [^{11}C]**M4K2127**, showed high initial brain uptake (SUV ∼ 2), including in the region of interest (pons). This data supports the use of this chemotype as a brain penetrant ALK2 inhibitor that permeates evenly into the pons with potential application for the treatment of DIPG.

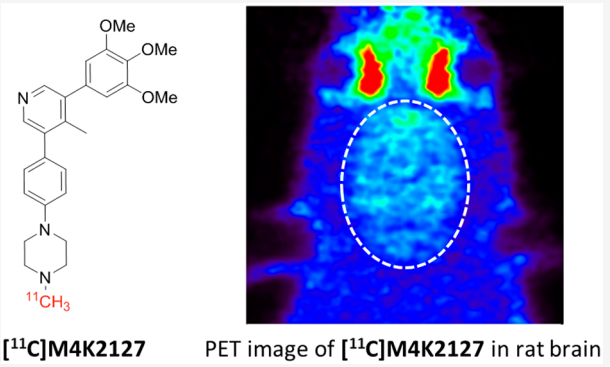

[^{11}C]**M4K2127** PET image of [^{11}C]**M4K2127** in rat brain

KEYWORDS: *Carbon-11, Positron emission tomography, ALK2, DIPG, Blood-brain barrier*

Activin receptor-like kinase 2 (ALK2) is a kinase receptor encoded by the ACVR1 gene. Mutations in ACVR1 causing a gain-of-function in ALK2 signaling have been reported in approximately 25−30% of children with diffuse intrinsic pontine glioma (DIPG), a rare pediatric brainstem cancer with a poor prognosis.[1−3] DIPG tumors are aggressive and arise from the brain's glial tissue in the lowest stem-like portion of the brain, the pons. Although the pathology of the relationship is not yet fully known, ALK2 has emerged as a potential therapeutic target for the treatment of DIPG. Kinase inhibitors have notoriously poor selectivity, often showing off-target affinity to other kinases within a family because of the high degree of structural homology in ATP binding domains. In the case of ALK2, off-target binding to the closely related TGFβ pathway receptor ALK5 is of specific concern due to potential cardiotoxicity.[4] In addition, the discovery of kinase inhibitors that are sufficiently able to cross the blood−brain barrier (BBB) has been lacking[5] and there is no report of work aiming to measure the degree of penetration of DIPG-directed therapeutics into the pons.[6−8] We recently reported on leveraging an open science drug discovery model[9] to synthesize a series of 3,5-diphenylpyridine ALK2-selective inhibitors that cross the BBB for the treatment of DIPG.[10,11] The lead compounds from this effort show brain penetration in rodent models with total brain to plasma (B/P) ratios of 0.8−1.4, although distribution into the therapeutic region of interest in the brain (pons) was unknown. Central nervous system (CNS) drug discovery can be facilitated with position emission tomography (PET) imaging by measuring the BBB permeability of isotopically labeled drug candidates. In addition, PET imaging can be used to visualize distribution of the radiotracer into specific regions of the brain such as the pons. In addition to our recent work on ALK2 drug discovery, the goal of the present study was to apply an open science approach for PET radiotracer discovery, to label four lead potent and ALK2-selective inhibitors with carbon-11 (half-life = 20.4 min), and to assess the BBB permeability of these radiotracers by PET imaging in rodent models. Assessment of the brain permeability of these compounds as PET radiotracers identified a candidate radioligand that can be used for further drug development of ALK2 inhibitors of this chemotype, facilitating receptor occupancy, target engagement, and dosing regimen studies.

Four lead compounds with IC_{50} values for ALK2 between 9−19 nM were selected for radiolabeling: **M4K2163**,

Received: March 2, 2021
Accepted: April 21, 2021
Published: April 23, 2021

https://doi.org/10.1021/acsmedchemlett.1c00127
ACS Med. Chem. Lett. 2021, 12, 846−850

M4K2009, **M4K2117**, and **M4K2127**.[11] The structural position of the ^{11}C radionuclide was chosen based on availability of the desmethyl precursors and ease of synthesis (Figure 1). While there is no consensus for the ideal

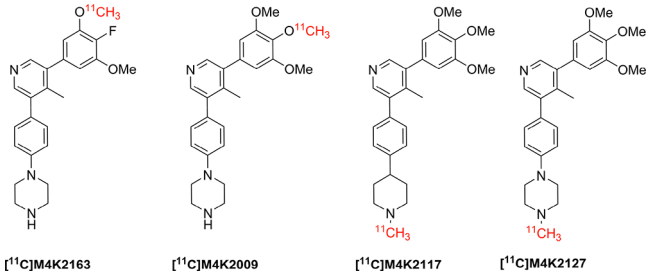

Figure 1. Structures of our lead ^{11}C-radiotracers for ALK2.

physiochemical properties of small molecules that are BBB penetrant,[12] CNS Multiparameter Optimization (MPO) scores offer a guideline for compound prioritization.[13] Prior to radiolabeling, CNS MPO desirability scores were calculated for all of the lead compounds, giving scores of 4.34−5.04 (maximum score is 6.0), suggesting that all compounds are rational leads as brain-penetrant radioligands. Calculated $logD_{7.4}$ values were also within the range for most brain-penetrant PET radioligands[14,15] (2.03−3.31), with limited off-target binding. As such, none of the initially identified compounds were excluded due to physiochemical characteristics that would suggest low brain permeability (Table 1).

All radiosyntheses were performed on a commercial automated carbon-11 synthesis unit for methylation reactions (GE FX2 C). [^{11}C]**M4K2163** and [^{11}C]**M4K2009** were synthesized by ^{11}C-*O*-methylation with the "loop method"[16,17] using $[^{11}C]CH_3I$ and the respective phenolic precursors (**M4K2297** and **M4K2298**; see the Supporting Information for their preparation) with <1 equiv of potassium *tert*-butoxide (Scheme 1A). The radioligands were synthesized, isolated, and formulated in radiochemical yields of 6−10% ([^{11}C]**M4K2163**, n = 3) and 4−9% ([^{11}C]**M4K2009**, n = 2) relative to $[^{11}C]CO_2$. Both radiotracers were obtained in >95% radiochemical purities and high molar activities ([^{11}C]**M4K2163**: 270−350 GBq/μmol), [^{11}C]**M4K2009**: 304 GBq/μmol). Small-scale vial-based radiosyntheses of [^{11}C]**M4K2117** and [^{11}C]**M4K2127** using $[^{11}C]CH_3I$ and various bases (KO*t*Bu, NaOH, or TBAOH) resulted in low radiochemical conversion (<5%) by analytical HPLC and were not further pursued. [^{11}C]**M4K2117** and [^{11}C]**M4K2127** were each synthesized by ^{11}C-*N*-methylation and also with use of the "loop method", although synthesis of these radioligands employed the more reactive $[^{11}C]CH_3OTf$ and the respective *N*-desmethyl precursors (**M4K2009** and **M4K2043**, Scheme 1B). For the efficient radiolabeling of [^{11}C]**M4K2117**, 1 equiv of aqueous NaOH was added to the reaction mixture. These radioligands were synthesized, isolated, and formulated in radiochemical yields of 5−6% ([^{11}C]**M4K2117**, n = 3) and 11−26% ([^{11}C]**M4K2127**, n = 5) relative to $[^{11}C]CO_2$. Both radiotracers were obtained in >99% radiochemical purities and high molar activities ([^{11}C]**M4K2117**: 269 GBq/μmol), [^{11}C]**M4K2127**: 132−664 GBq/μmol). All radiotracers were prepared within 30−40 min from end of bombardment.

Scheme 1. Radiosynthesis of ^{11}C-Labeled Compounds[a]

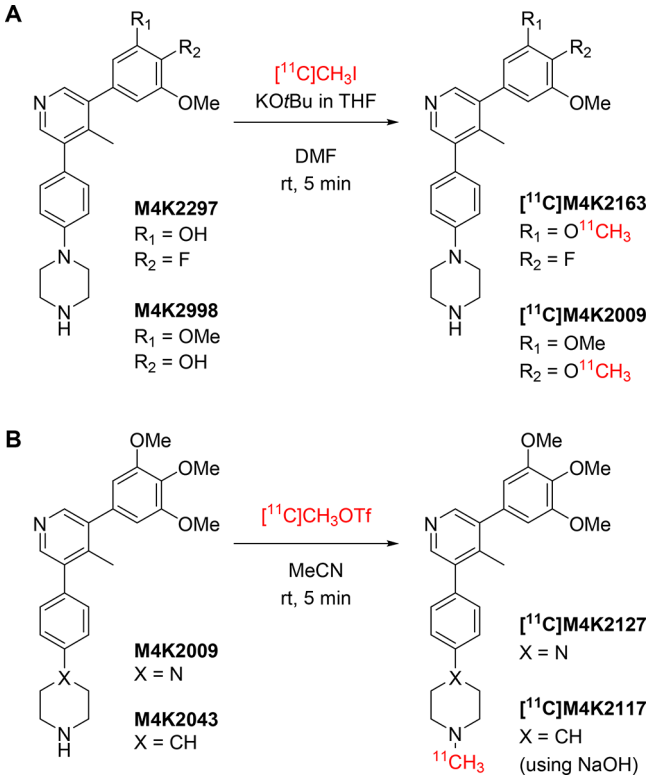

[a](A) *O*-methylations *via* $[^{11}C]CH_3I$, (B) *N*-methylations *via* $[^{11}C]CH_3OTf$.

Shake-flask $logD_{7.4}$ values were experimentally determined using established procedures.[18] Aliquots of the formulated radiotracers were partitioned between octanol/phosphate buffer, and the radioactivity in each layer was measured on a γ counter. Experimental $logD_{7.4}$ values were slightly higher than the calculated values and were in the range of 2.45−3.37 (Table 1), consistent with most CNS PET tracers.[14,15]

The brain permeability of the radiotracers was then assessed in healthy Sprague−Dawley rats (Figure 2). Rats were injected (*i.v.*; tail-vein) with 16−23 MBq of each radiotracer, and dynamic PET imaging was acquired over 90 min. Time-activity

Table 1. Physiochemical Properties of the Lead Compounds

	ALK2 IC_{50} (nM)[a]	B/P[b]	pK_a[c]	clogP[c]	$clogD_{7.4}$[c]	$logD_{7.4}$[d]	CNS MPO[e]
M4K2009	13	0.9*	8.5	3.20	2.03	2.76 ± 0.13	5.04
M4K2117	7	0.82	9.5	4.56	2.46	2.64 ± 0.05	4.34
M4K2127	9		7.6	3.74	3.31	3.37 ± 0.12	4.34
M4K2163	19	1.41	8.5	4.05	2.88	2.45 ± 0.04	4.34

[a]Cellular IC_{50}.[11] [b]Brain/plasma ratio in female SCID mice (4 h) or *male SD-1 mice (2 h) @ 10 mg/kg PO.[11] [c]Properties retrieved from ACD/I-Lab 2.0. [d]Determined experimentally by shake-flask method with ^{11}C-labeled compounds. [e]Scored via an algorithm using a weighted scoring function for clogP, clogD, molecular weight, topological polar surface area, HBDs, and pK_a.

https://doi.org/10.1021/acsmedchemlett.1c00127
ACS Med. Chem. Lett. 2021, 12, 846−850

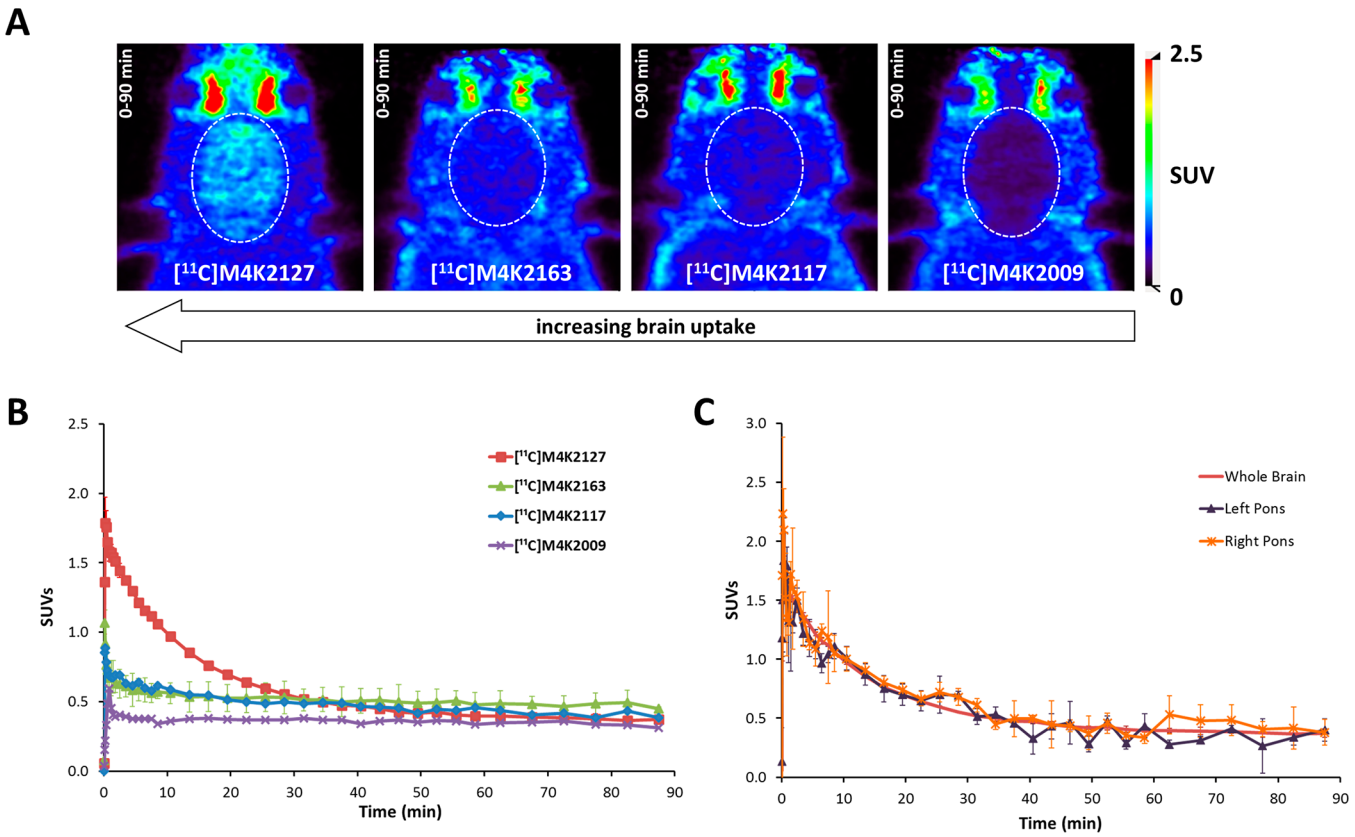

Figure 2. (A) Summed (0−90 min, iterative reconstruction) PET images in transverse plane for the four ^{11}C-radiotracers in male SD rats. (B) Whole brain TACs for the radiotracers (0−90 min). (C) TACs for the pons for [^{11}C]**M4K2127** (0−90 min, n = 3).

curves (TACs) were extracted for whole brain and for the pons as a region of interest using the atlas of Schwarz et al. 2006[19] implemented in VivoQuant (4.0patch1, Invicro). Three tracers, [^{11}C]**M4K2163** (n = 2), [^{11}C]**M4K2117** (n = 1), and [^{11}C]**M4K2009** (n = 1) showed relatively low brain uptake, with peak SUV values of 1.1, 0.9, and 0.6, respectively, within 1 min after injection. Fortunately, [^{11}C]**M4K2127** (n = 3) showed good permeability into the brain, with a peak SUV of 1.8 ± 0.2 for initial brain uptake within 1 min after injection, followed by a moderate rate of wash out over 30 min. Importantly, we found that [^{11}C]**M4K2127** has high uptake in the pons (peak SUV = 2.0 ± 0.3). Looking at the similar TACs for [^{11}C]**M4K2127** in the pons and the whole brain, it is evident the compound permeates homogeneously into the pons as compared to the rest of the brain. This, importantly, constitutes the first example of an ALK2 PET radiotracer and provides evidence that compounds of this chemotype can access the pons, which is the specific region of interest for the treatment of DIPG tumors.

To investigate the properties that could be affecting the BBB permeability of these four compounds, we reviewed their Caco-2 permeability parameters as an indication of membrane permeability as well as to consider the compounds as potential substrates of efflux transporters. As anticipated from the PET imaging results, **M4K2127** had the highest Caco-2 permeability, three times greater than that of **M4K2009** ($P_{app\ AB}$ = 16.6 vs 5.4 × 10^{-6} cm/s where P_{app} > 3 indicates high permeability). Additionally, the efflux ratio for **M4K2127** was found to be almost 2−3-fold better than that of **M4K2009** and **M4K2163** (efflux ratio BA/AB = 0.9, 1.5, and 2.7, respectively; see the Supporting Information, Table S1). This could be attributed to the lower pK_a of the *N*-methyl piperazine moiety in **M4K2127** (Table 1) along with the molecule having a reduced number of hydrogen bond donors (HBDs), a parameter often associated with a decrease in permeability glycoprotein (P-gp)-mediated efflux.[12] Among the four lead compounds, **M4K2127** showed the lowest microsomal stability (see the Supporting Information, Table S1), which is a potential hurdle for further development as a drug candidate. However, when administered via *i.v.* injection as in our rodent PET imaging study, **M4K2127** initially avoids major first-pass metabolism by the liver which increases the initial Cmax. These *in vitro* ADME results align well with the PET imaging data demonstrating that [^{11}C]**M4K2127**, having the best permeability *in vitro*, efficiently crosses the BBB.

Herein, we present [^{11}C]**M4K2127** as an ALK2-targeting radioligand that satisfactorily and homogeneously permeates the brain. By employing an open science approach to this work, we were able to rapidly radiolabel isotopologs of our lead ALK2 inhibitors and apply PET imaging for the assessment of brain penetration. The present study sheds light on our previous work to establish *B*/*P* ratios in this new class of ALK2 inhibitors,[11] with implications both for the drug development process and direct analysis of DIPG-targeting drug candidates in a clinical setting. To our knowledge, this report constitutes the first disclosure of ALK2 PET radiotracers and efforts aimed at assessing the degree of penetration into the brain (including the pons) of a compound being pursued as a potential treatment for DIPG.[20]

While numerous compounds have entered the clinic for DIPG, no studies on their degree of penetration into the pons (using PET imaging, or any other method) have been

https://doi.org/10.1021/acsmedchemlett.1c00127
ACS Med. Chem. Lett. 2021, 12, 846−850

reported. [^{11}C]**M4K2127** will be used as a biomarker to further assist the drug development of 3,5-diphenylpyridine ALK2 inhibitors. Blocking studies with [^{11}C]**M4K2127** to confirm specific binding in the brain of rodents and higher species, evaluation of radiometabolism, and effect of anesthesia are planned. [^{11}C]**M4K2127** may also be used as a tool in receptor occupancy, target engagement, and dosing regimens for other ALK2 inhibitors as they progress toward the clinic.

■ ASSOCIATED CONTENT

Supporting Information

The Supporting Information is available free of charge at https://pubs.acs.org/doi/10.1021/acsmedchemlett.1c00127.

Details for the synthesis and characterization of M4K2127, M4K2117, M4K2297, and M4K2298; details for the radiochemical synthesis and characterization of [^{11}C]M4K2009, [^{11}C]M4K2117, [^{11}C]M4K2127, and [^{11}C]M4K2163; protocols for logD7.4 measurement and *in vivo* animal PET/MR imaging ADME parameters for ALK2 inhibitors and ADME assay protocols (DOCX)

■ AUTHOR INFORMATION

Corresponding Authors

Iain D. G. Watson − *Drug Discovery Program, Ontario Institute for Cancer Research, M5G 0A3 Toronto, Ontario, Canada;* orcid.org/0000-0003-3508-3240; Email: iain.watson@oicr.on.ca

Neil Vasdev − *Azrieli Centre for Neuro-Radiochemistry, Brain Health Imaging Centre, Centre for Addiction and Mental Health (CAMH), M5T 1R8 Toronto, Ontario, Canada; Department of Psychiatry, University of Toronto, M5T 1R8 Toronto, Ontario, Canada;* orcid.org/0000-0002-2087-5125; Email: neil.vasdev@utoronto.ca

Authors

Emily Murrell − *Azrieli Centre for Neuro-Radiochemistry, Brain Health Imaging Centre, Centre for Addiction and Mental Health (CAMH), M5T 1R8 Toronto, Ontario, Canada*

Junchao Tong − *Azrieli Centre for Neuro-Radiochemistry, Brain Health Imaging Centre, Centre for Addiction and Mental Health (CAMH), M5T 1R8 Toronto, Ontario, Canada*

David Smil − *Drug Discovery Program, Ontario Institute for Cancer Research, M5G 0A3 Toronto, Ontario, Canada;* orcid.org/0000-0002-6232-6087

Taira Kiyota − *Drug Discovery Program, Ontario Institute for Cancer Research, M5G 0A3 Toronto, Ontario, Canada*

Ahmed M. Aman − *Drug Discovery Program, Ontario Institute for Cancer Research, M5G 0A3 Toronto, Ontario, Canada; Leslie Dan Faculty of Pharmacy, University of Toronto, M5S 3M2 Toronto, Ontario, Canada*

Methvin B. Isaac − *Drug Discovery Program, Ontario Institute for Cancer Research, M5G 0A3 Toronto, Ontario, Canada*

Complete contact information is available at: https://pubs.acs.org/10.1021/acsmedchemlett.1c00127

Author Contributions

The manuscript was written by E.M. and edited with D.S., I.D.G.W., and N.V., including contributions by all authors. Radiochemical tracers were synthesized by E.M. with precursors synthesized by D.S. (**M4K2127**, **M4K2117**, and **M4K2297**) and I.D.G.W. (**M4K2298**). Radiochemical tracer compounds were designed, and their syntheses were devised by E.M. and N.V. The precursor compounds were designed, and their syntheses were devised by D.S. and I.D.G.W. Caco-2 HRMS and microsomal stability studies for **M4K2127** were conducted by T.K. Animal and imaging studies were performed by J.T including image analysis. E.M., I.D.G.W., and N.V. conceived and initiated the project. All authors have given approval to the final version of the manuscript.

Funding

N.V. thanks the Azrieli Foundation and the Canada Research Chairs Program, Canada Foundation for Innovation, and the Ontario Research Fund for support. The Ontario Institute for Cancer Research (OICR) receives financial support from the Government of Ontario through the Ministry of Training, Colleges, and Universities.

Notes

The authors declare no competing financial interest.

■ ACKNOWLEDGMENTS

M4K Pharma Inc., functioning as a virtual biotech, serves as a *de facto* hub for gathering and aligning the cooperation and contributions of academic and industry partners into a drug development program that operates free of restrictions on data disclosure (i.e., no patents are filed). The authors thank the scientific leadership of M4K Pharma, Dr. Aled M. Edwards, Dr. Peter Ho, and Owen G. Roberts, for encouraging and supporting our open science research collaboration. We thank all members of the Azrieli Centre for Neuro-Radiochemistry and the CAMH Brain Health Imaging Centre for support with the cyclotron, radiochemistry, methodology, and imaging.

■ ABBREVIATIONS

ADME, absorption distribution metabolism excretion; ALK2, activin-like receptor 2; BBB, blood−brain barrier; *B/P*, total brain-to-plasma ratio; CNS, central nervous system; DIPG, diffuse intrinsic pontine glioma; HBD, hydrogen bond donor; MPO, multiparameter optimization; PET, positron emission tomography; rt, room temperature; SUV, standard uptake value; TAC, time−activity curve

■ REFERENCES

(1) Taylor, K. R.; Vinci, M.; Bullock, A. N.; Jones, C. ACVR1Mutations in DIPG: Lessons Learned from FOP. *Cancer Res.* **2014**, *74* (17), 4565−4570.

(2) Pacifici, M.; Shore, E. M. Common Mutations in ALK2/ACVR1, a Multi-Faceted Receptor, Have Roles in Distinct Pediatric Musculoskeletal and Neural Orphan Disorders. *Cytokine Growth Factor Rev.* **2016**, *27*, 93−104.

(3) Taylor, K. R.; Mackay, A.; Truffaux, N.; Butterfield, Y.; Morozova, O.; Philippe, C.; Castel, D.; Grasso, C. S.; Vinci, M.; Carvalho, D.; Carcaboso, A. M.; de Torres, C.; Cruz, O.; Mora, J.; Entz-Werle, N.; Ingram, W. J.; Monje, M.; Hargrave, D.; Bullock, A. N.; Puget, S.; Yip, S.; Jones, C.; Grill, J. Recurrent Activating ACVR1Mutations in Diffuse Intrinsic Pontine Glioma. *Nat. Genet.* **2014**, *46* (5), 457−461.

(4) Herbertz, S.; Sawyer, J. S.; Stauber, A. J.; Gueorguieva, I.; Driscoll, K. E.; Estrem, S. T.; Cleverly, A. L.; Desaiah, D.; Guba, S. C.; Benhadji, K. A.; Slapak, C. A.; Lahn, M. M. Clinical Development of Galunisertib (LY2157299 Monohydrate), a Small Molecule Inhibitor of Transforming Growth Factor-Beta Signaling Pathway. *Drug Des., Dev. Ther.* **2015**, *9*, 4479−4499.

(5) Heffron, T. P. Small Molecule Kinase Inhibitors for the Treatment of Brain Cancer. *J. Med. Chem.* **2016**, *59* (22), 10030−10066.
(6) Green, A. L.; Flannery, P.; Hankinson, T. C.; O'Neill, B.; Amani, V.; DeSisto, J.; Knox, A.; Chatwin, H.; Lemma, R.; Hoffman, L. M.; Mulcahy Levy, J.; Raybin, J.; Hemenway, M.; Gilani, A.; Koschmann, C.; Dahl, N.; Handler, M.; Pierce, A.; Venkataraman, S.; Foreman, N.; Vibhakar, R.; Wempe, M. F.; Dorris, K. Preclinical and Clinical Investigation of Intratumoral Chemotherapy Pharmacokinetics in DIPG Using Gemcitabine. *Neuro-oncology Adv.* **2020**, *2* (1), vdaa021−vdaa021.
(7) Srikanthan, D.; Taccone, M. S.; Van Ommeren, R.; Ishida, J.; Krumholtz, S. L.; Rutka, J. T. Diffuse Intrinsic Pontine Glioma: Current Insights and Future Directions. *Chinese Neurosurg. J.* **2021**, *7* (1), 6.
(8) Subashi, E.; Cordero, F. J.; Halvorson, K. G.; Qi, Y.; Nouls, J. C.; Becher, O. J.; Johnson, G. A. Tumor Location, but Not H3.3K27M, Significantly Influences the Blood-Brain-Barrier Permeability in a Genetic Mouse Model of Pediatric High-Grade Glioma. *J. Neuro-Oncol.* **2016**, *126* (2), 243−251.
(9) Morgan, M. R.; Roberts, O. G.; Edwards, A. M. Ideation and Implementation of an Open Science Drug Discovery Business Model - M4K Pharma. *Wellcome open Res.* **2018**, *3*, 154.
(10) Ensan, D.; Smil, D.; Zepeda-Velázquez, C. A.; Panagopoulos, D.; Wong, J. F.; Williams, E. P.; Adamson, R.; Bullock, A. N.; Kiyota, T.; Aman, A.; Roberts, O. G.; Edwards, A. M.; O'Meara, J. A.; Isaac, M. B.; Al-awar, R. Targeting ALK2: An Open Science Approach to Developing Therapeutics for the Treatment of Diffuse Intrinsic Pontine Glioma. *J. Med. Chem.* **2020**, *63* (9), 4978−4996.
(11) Smil, D.; Wong, J. F.; Williams, E. P.; Adamson, R. J.; Howarth, A.; McLeod, D. A.; Mamai, A.; Kim, S.; Wilson, B. J.; Kiyota, T.; Aman, A.; Owen, J.; Poda, G.; Horiuchi, K. Y.; Kuznetsova, E.; Ma, H.; Hamblin, J. N.; Cramp, S.; Roberts, O. G.; Edwards, A. M.; Uehling, D.; Al-awar, R.; Bullock, A. N.; O'Meara, J. A.; Isaac, M. B. Leveraging an Open Science Drug Discovery Model to Develop CNS-Penetrant ALK2 Inhibitors for the Treatment of Diffuse Intrinsic Pontine Glioma. *J. Med. Chem.* **2020**, *63* (17), 10061−10085.
(12) Rankovic, Z. CNS Drug Design: Balancing Physicochemical Properties for Optimal Brain Exposure. *J. Med. Chem.* **2015**, *58* (6), 2584−2608.
(13) Wager, T. T.; Hou, X.; Verhoest, P. R.; Villalobos, A. Central Nervous System Multiparameter Optimization Desirability: Application in Drug Discovery. *ACS Chem. Neurosci.* **2016**, *7* (6), 767−775.
(14) Waterhouse, R. N. Determination of Lipophilicity and Its Use as a Predictor of Blood−Brain Barrier Penetration of Molecular Imaging Agents. *Mol. Imaging Biol.* **2003**, *5* (6), 376−389.
(15) Pike, V. W. PET Radiotracers: Crossing the Blood−Brain Barrier and Surviving Metabolism. *Trends Pharmacol. Sci.* **2009**, *30* (8), 431−440.
(16) Wilson, A. A.; Garcia, A.; Jin, L.; Houle, S. Radiotracer Synthesis from [11C]-Iodomethane: A Remarkably Simple Captive Solvent Method. *Nucl. Med. Biol.* **2000**, *27* (6), 529−532.
(17) Wilson, A. A.; Garcia, A.; Houle, S.; Vasdev, N. Utility of Commercial Radiosynthetic Modules in Captive Solvent [11C]-Methylation Reactions. *J. Labelled Compd. Radiopharm.* **2009**, *52* (11), 490−492.
(18) Wilson, A. A.; Jin, L.; Garcia, A.; DaSilva, J. N.; Houle, S. An Admonition When Measuring the Lipophilicity of Radiotracers Using Counting Techniques. *Appl. Radiat. Isot.* **2001**, *54* (2), 203−208.
(19) Schwarz, A. J.; Danckaert, A.; Reese, T.; Gozzi, A.; Paxinos, G.; Watson, C.; Merlo-Pich, E. V.; Bifone, A. A Stereotaxic MRI Template Set for the Rat Brain with Tissue Class Distribution Maps and Co-Registered Anatomical Atlas: Application to Pharmacological MRI. *NeuroImage* **2006**, *32* (2), 538−550.
(20) Lin, G. L.; Wilson, K. M.; Ceribelli, M.; Stanton, B. Z.; Woo, P. J.; Kreimer, S.; Qin, E. Y.; Zhang, X.; Lennon, J.; Nagaraja, S.; Morris, P. J.; Quezada, M.; Gillespie, S. M.; Duveau, D. Y.; Michalowski, A. M.; Shinn, P.; Guha, R.; Ferrer, M.; Klumpp-Thomas, C.; Michael, S.; McKnight, C.; Minhas, P.; Itkin, Z.; Raabe, E. H.; Chen, L.; Ghanem, R.; Geraghty, A. C.; Ni, L.; Andreasson, K. I.; Vitanza, N. A.; Warren, K. E.; Thomas, C. J.; Monje, M. Therapeutic Strategies for Diffuse Midline Glioma from High-Throughput Combination Drug Screening. *Sci. Transl. Med.* **2019**, *11* (519), eaaw0064.

https://doi.org/10.1021/acsmedchemlett.1c00127
ACS Med. Chem. Lett. 2021, 12, 846−850